

MS-Diffusion: Multi-subject Zero-shot Image Personalization with Layout Guidance*

X. Wang^{1,2,+} Siming Fu^{1,+} Qihan Huang^{1,2} Wanggui He¹ Hao Jiang^{1,†}

¹Alibaba Group ²Zhejiang University

⁺Equal contribution [†]Corresponding author

<https://MS-Diffusion.github.io>



Figure 1: Representative outputs showcase the capabilities of MS-Diffusion in typical applications. The MS-Diffusion framework facilitates personalization across both single-subject scenarios (the upper panel) and multi-subject contexts (the lower panel). Notably, while preserving the intricacies of subject detail, MS-Diffusion achieves a marked enhancement in textual fidelity.

Abstract

Recent advancements in text-to-image generation models have dramatically enhanced the generation of photorealistic images from textual prompts, leading to an increased interest in personalized text-to-image applications, particularly in multi-subject scenarios. However, these advances are hindered by two main challenges: firstly, the need to accurately maintain the details of each referenced subject in accordance with the textual descriptions; and secondly, the difficulty in achieving a cohesive representation of multiple subjects in a single image without introducing inconsistencies. To address these concerns, our research introduces the MS-Diffusion framework for layout-guided zero-shot image personalization with

*Work done during internship of X. Wang and Q. Huang at Alibaba Group.

multi-subjects. This innovative approach integrates grounding tokens with the feature resampler to maintain detail fidelity among subjects. With the layout guidance, MS-Diffusion further improves the cross-attention to adapt to the multi-subject inputs, ensuring that each subject condition acts on specific areas. The proposed multi-subject cross-attention orchestrates harmonious inter-subject compositions while preserving the control of texts. Comprehensive quantitative and qualitative experiments affirm that this method surpasses existing models in both image and text fidelity, promoting the development of personalized text-to-image generation.

1 Introduction

Recent advancements in text-to-image (T2I) diffusion methodologies [3, 27, 29] have propelled the field to new heights, realizing unprecedented levels of photorealism while demonstrating a refined ability to conform to textual prompts. These achievements have spurred the development of a broad spectrum of applications, most prominently in the domain of personalized T2I (P-T2I) models, which are tasked with the complex undertaking of assimilating and regenerating novel visual concepts or subjects across diverse contexts with a heightened demand for conceptual and compositional fidelity. Despite fine-tuning-based techniques such as DreamBooth [28] and Textual Inversion [9] yield results with considerable accuracy, they necessitate extensive resources for tuning individual instances and for the storage of multiple models, which renders them less feasible for widespread application. To circumvent these resource-intensive requirements, fine-tuning-free alternatives have come to the fore.

Single-subject driven personalization methods, IP-Adapter [38] and ELITE [36] for instance, introduce a specialized cross-attention mechanism that distinctly processes text and image features, thereby affording the possibility to employ reference images directly as visual prompts within the model. Furthermore, recent works have employed multi-subject driven customization methodologies to concatenate visual concepts with textual prompts, offering a glimpse of the potential in techniques like SSR-Encoder [40], λ -ECLIPSE [20], Emu2 [30], and KOSMOS-G [19]. These models harness identity data and amalgamate it with text via cross-attention, exhibiting proficiency in adjusting textures. Nevertheless, above zero-shot personalization methods encounter limitations, notably in adapting a pressing question pertains to the congruence of granular details between the subject depicted in the synthesized imagery and its corresponding subjects, along with the degree of semblance between the content of the generated image and associated textual descriptions. The challenge is further amplified in scenarios requiring the personalization of multiple subjects. Especially, the challenge of ensuring harmonious representation when multiple subjects are incorporated—specifically, the elucidation of whether the resultant image manifests any discordant elements or deleterious interactions in accordance with textual directives and multi-subject referential controls. As illustrated in Figure 2, multi-subject personalization methods frequently incur notable detail inaccuracies in a fine-tuning-free framework and often lead to subject neglect, subject overcontrol, and subject-subject conflict issue within the generated images.

To confront these identified challenges, we are the **first** to introduce the layout-guided zero-shot image personalization with multiple subjects (MS-Diffusion) framework, which consolidates the accommodation of multiple subjects, the incorporation of zero-shot learning capabilities, the provision of layout guidance, and the preservation of the foundational model’s parameters. Firstly, we design the grounding resampler to extract the subject detailed features and integrate them with grounding information containing entities and boxes. As an image projection module, the proposed grounding resampler can enhance the subject fidelity while appending semantic and positional priors. Secondly, we propose a novel cross-attention mechanism for multiple subjects, which confines subjects to represent themselves in specific areas. This confluence not only facilitates the efficacious infusion of multi-subject data into the model but also mitigates conflicts between text and image subject control conditions. Such an approach culminates in the refined granularity of control over the image’s multi-subject composition. The experimental results demonstrate our method consistently outperforms the state-of-the-art approaches on all the benchmarks. **We conclude the previous P-T2I works and provide an overall comparison in Table 1.** The contributions can be summarized as follows:

- We introduce a layout-guided, zero-shot multi-subject image personalization framework within the diffusion model paradigm, designated as ‘MS-Diffusion’. This innovation stream-

Table 1: **An overview of previous studies of P-T2I tasks.** MS-Diffusion is the **first** approach to support multi-reference zero-shot P-T2I generation with layout guidance and base model freezing.

| Method | Zero Shot | Multi Subject | Base Model Freezing | MLLM Free | Layout Guidance |
|-------------------------|-----------|---------------|---------------------|-----------|-----------------|
| Textual Inversion [9] | ✗ | ✗ | ✓ | ✓ | ✗ |
| DreamBooth [28] | ✗ | ✗ | ✗ | ✓ | ✗ |
| ELITE [36] | ✓ | ✗ | ✗ | ✓ | ✗ |
| BLIP-Diffusion [15] | ✓ | ✗ | ✗ | ✗ | ✗ |
| IP-Adapter [38] | ✓ | ✗ | ✓ | ✓ | ✗ |
| Ēmu2 [30] | ✓ | ✓ | ✗ | ✗ | ✗ |
| Kosmos-G [19] | ✓ | ✓ | ✓ | ✗ | ✗ |
| λ -ECLIPSE [20] | ✓ | ✓ | ✓ | ✗ | ✗ |
| SSR-Encoder [40] | ✓ | ✓ | ✓ | ✓ | ✗ |
| MS-Diffusion | ✓ | ✓ | ✓ | ✓ | ✓ |

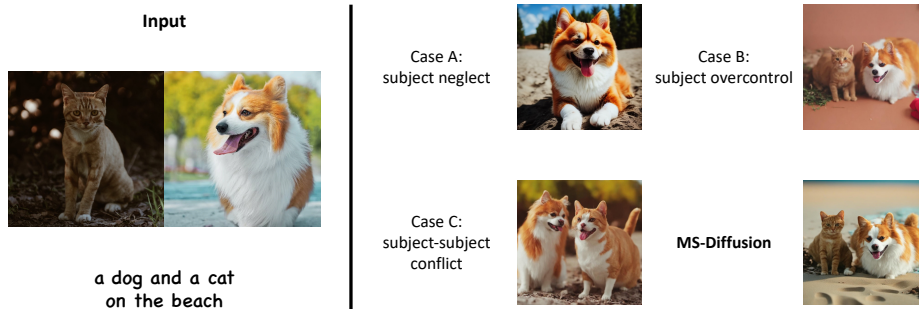


Figure 2: **Challenges inherent in multi-subject personalization approaches.** Through the explicit layout guidance, MS-Diffusion addresses these challenges by directing subject conditioning to specific areas, simultaneously maintaining high image fidelity.

lines the complex process of preserving detailed subject references. Moreover, it seamlessly integrates multiple subjects into a coherent and harmonious personalized image.

- The 'Grounding Resampler' is advanced as a novel feature refinement mechanism. This construct enriches the detail extraction from images by ascertaining the correlative content and fusing it with box embeddings that demarcate the anticipated spatial zones for each subject. Additionally, we introduce a specialized multi-subject cross-attention mechanism, confronting and rectifying prevalent complications in multi-subject personalization, including inadvertent subject neglect, disproportionate subject dominance, and internecine subject conflicts.
- The capabilities of 'MS-Diffusion' are empirically substantiated through its ability to synthesize a broader spectrum of images with notable fidelity. The paper further delineates comprehensive ablation studies, underpinning the rationale behind our design decisions and affirming the efficacy of our proposed approach.

2 Related Work

2.1 Text-to-image Generation

Text-to-image generative models [2, 3, 27, 29] are capable of producing high-quality images using user-provided text prompts. In recent times, diffusion-based models have shown strong performance in text-to-image tasks. Stable Diffusion [27] proposes conducting the diffusion process in latent space rather than pixel space, which reduces the sampling steps without compromising image quality. Kandinsky [26] takes both text embedding and image embedding as conditions to generate images

more controllably. DALLE-3 [3] recaptions the training data pairs and utilizes T5-XXL [7] as the text encoder to strengthen the prompt-following ability. StableCascade [22] presents a cascaded architecture to leverage outputs of front stages as priors, further reducing the latent space. PixArt- α [5] also employs a large T5 text encoder and replaces the original U-Net backbone with a transformer [21]. These models focus on the basic text-to-image ability and cannot handle the situation when users provide specific subjects.

To finely control text-to-image generation, some diffusion models [17, 35, 41] support users in providing layout guidance. Layout Diffusion [41] and GLIGEN [17] input positions and labels of bounding boxes into the diffusion model and train it to learn the layout information. DenseDiffusion [12] develops a training-free method and modulates the attention maps in the inference phase. Instance Diffusion [34] and MIGC [42] extend the layout-conditioned diffusion to the instance level, enabling the model to generate multiple objects with precise quantities. While layout-guided diffusion models have robust controllability, they cannot reference specific concepts, which is emphasized in personalized text-to-image generation.

2.2 Text-to-image Personalization

Text-to-image personalization [9, 10, 14, 24, 28] has attracted much attention in the community for its powerful referencing capability of both text and image prompts. Textual inversion [9] and DreamBooth [28] utilize an identifier in the text to bind the visual concept through fine-tuning. IP-Adapter [38] proposes a zero-shot personalized model by projecting the image embedding to the cross-attention layers. InstanceID [33] develops an approach for identity personalization, replacing the image encoder with a face encoder and employing ControlNet [39] to integrate the face landmarks. To narrow the gap between image and text prompts, Kosmos-G [19] and λ -ECLIPSE [20] conduct multi-modal training to unite the inputs by text-image interleaving. SSR-Encoder [40] design a query network to extract a single subject from images with multiple subjects for personalization.

Though past research in this field has significantly enhanced the ability to reference single subjects, few zero-shot multi-subject personalized models. Moreover, existing related works struggle to address conflicts in personalized generation with multiple subjects and generate bad results, which is precisely the focus of our work, to discuss and resolve these issues.

3 Method

The pipeline of MS-Diffusion is shown in Figure 3. Through an improved data construction strategy, we can get multiple subject images together with the corresponding entities and layouts as input. We propose a grounding resampler to separately extract the image features and integrate them with phrase embedding and box embedding for condition enhancement. Inside the cross-attention layers, we further introduce the masked cross-attention to guide the generation with layout priors and alleviate conflicts of multiple subjects. The training needs no pre-trained weights to be optimized and remains plug-and-play in various base models.

3.1 Preliminaries

Stable Diffusion with Image Prompt. As a widely used diffusion model, Stable Diffusion (SD) [27] conducts the diffusion process in the latent space. Given an image and a text prompt, SD encodes them into latent code \mathbf{z} and condition embedding \mathbf{c}_t utilizing VAE [32] and CLIP [25] text encoder, respectively. In zero-shot image personalization architectures like IP-adapter [38], images can also be considered a condition of the diffusion model. Specifically, a subject image is encoded to image embeddings by an image encoder and then projected into the original condition space of the diffusion model denoted as \mathbf{c}_i . For a timestep t which is uniformly sampled from a fixed range, the model θ predicts the noise ϵ_θ and is optimized through the objective:

$$\mathcal{L}_{IP} = \mathbb{E}_{\mathbf{z}, \mathbf{c}, \epsilon, t} \left[\|\epsilon - \epsilon_\theta(\mathbf{z} \mid \mathbf{c}_t, \mathbf{c}_i, t)\|_2^2 \right] \quad (1)$$

where $\epsilon \sim \mathcal{N}(\mathbf{0}, \mathbf{I})$. In this work, we employ \mathcal{L}_{IP} with SDXL [23] as the pre-trained model, which contains two CLIP text encoders and additional condition inputs besides \mathbf{c} and t , omitted for brevity.

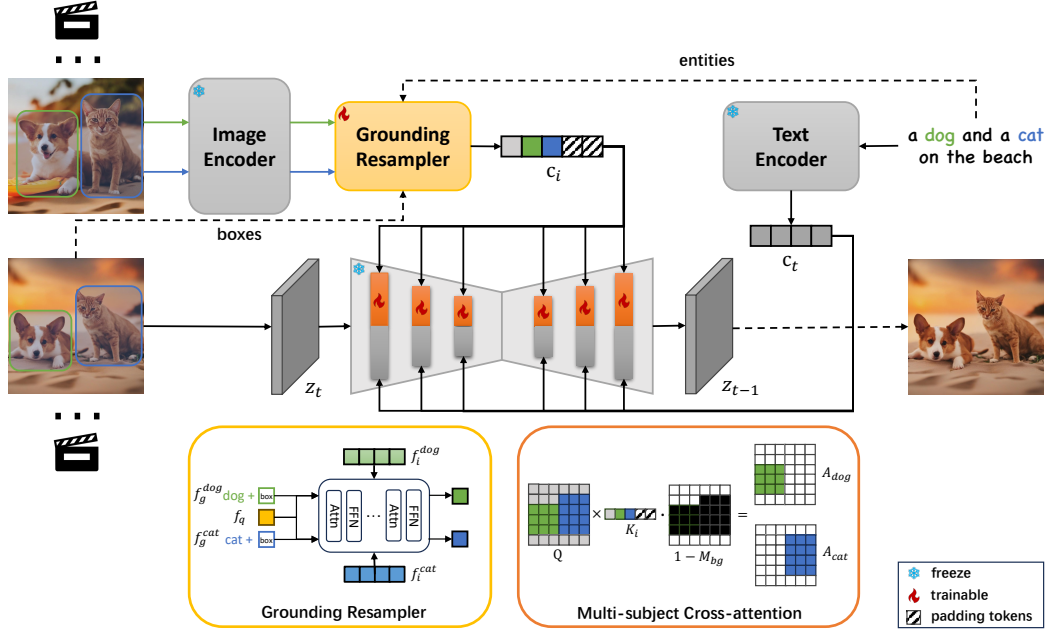


Figure 3: **The overall pipeline of MS-Diffusion.** It introduces two pivotal enhancements to the model: the grounding resampler and multi-subject cross-attention mechanisms. Firstly, the grounding resampler adeptly assimilates visual information, correlating it with specific entities and spatial constraints. Subsequently, a targeted cross-attention mechanism facilitates precise interactions between the image condition and the diffusion latent within the multi-subject attention layers. Throughout the training phase, all components of the pre-existing diffusion model remain frozen.

Cross-attention. In SD [27], both c_i and c_t are integrated into the U-Net backbone through cross-attention layers:

$$\text{Attn}(\mathbf{Q}, \mathbf{K}_i, \mathbf{K}_t, \mathbf{V}_i, \mathbf{V}_t) = \gamma \cdot \mathbf{z}_{img} + \mathbf{z}_{txt} = \gamma \cdot \text{Softmax}\left(\frac{\mathbf{Q}\mathbf{K}_i}{\sqrt{d}}\right) \mathbf{V}_i + \text{Softmax}\left(\frac{\mathbf{Q}\mathbf{K}_t}{\sqrt{d}}\right) \mathbf{V}_t \quad (2)$$

where $\mathbf{Q} = \mathbf{z}W_q$, $\mathbf{K}_i = \mathbf{c}_iW_k^i$, $\mathbf{K}_t = \mathbf{c}_tW_k^t$, $\mathbf{V}_i = \mathbf{c}_iW_v^i$, $\mathbf{V}_t = \mathbf{c}_tW_v^t$, and W_q, W_k, W_v are corresponding projection weight matrices. And d represents the dimensionality of the key vectors. Note that the key and value matrix of c_i and c_t are independent of each other to decouple conditions of different modalities. Previous studies [11, 31] have found that attention maps $\mathbf{A} = \text{Softmax}\left(\frac{\mathbf{Q}\mathbf{K}}{\sqrt{d}}\right)$ can reflect the attribution relation between generated images and conditions, which means that they determine the effect of condition controls.

3.2 Data Construction

In the field of multi-subject personalization, creating a robust dataset architecture is a significant challenge, especially when no pre-existing dataset includes a variety of reference subjects with their validated truths. Our method starts with applying a Named Entity Recognition (NER) protocol to textual data to extract relevant entities. These entities are then used within a detection framework to define the corresponding bounding boxes. This step generates training samples that encompass a range of [*subjects, entities, spatial layouts*].

Previous studies have mostly created training examples from stand-alone images which is essentially a reconstruction task, leading the resulting models to favor replication, often resulting in 'copy-and-paste' artifacts [6]. To address this issue, our enhanced approach involves extracting subjects from a single video frame and using another frame from the same sequence as a reference for the truth. This technique effectively separates the personalized references from the target images. Due to possible variations in subjects between frames, we use a specialized subject-matching algorithm to ensure accurate matching. We provide a detailed description of this data processing pipeline in Section A.

3.3 Grounding Resampler

Different from text embedding, image embedding generally contains more information and is sparser, making projection into the condition space challenging. Leveraging embeddings from all image patches primarily control the condition, but the pooled output from the image encoder tends to omit many details. **Different from** [1] and [38], we propose the integration of a grounding resampler that functions as an alternative form of image projector. Utilizing a set of learnable tokens, the grounding resampler queries and distills pertinent information from the image features. Specifically, with an image embedding f_i and a learnable query f_q , the resampler comprises several attention layers:

$$\text{RSAttn} = \text{Softmax} \left(\frac{\mathbf{Q}(f_q) \mathbf{K}([f_i, f_q])}{\sqrt{d}} \right) \mathbf{V}([f_i, f_q]) \quad (3)$$

where $[f_i, f_q]$ denotes the concatenation of the image embedding f_i and the learnable query f_q . The architecture incorporates fully connected feedforward networks (FFNs), analogous to those utilized in standard vision transformers [8].

As detailed in 3.2, we can obtain entities of multiple referenced subjects and their target area boxes in the generated image. We present to initialize the query f_q with grounding tokens f_g derived from text embedding of entities and Fourier embedding of boxes. Entities are related to the semantic information of images and boxes indicate the areas where the subjects are supposed to be. *It would be helpful for the resampler to extract the image features appropriately and the cross-attention layers to condition the generation finely.* To prevent the model from becoming dependent on the grounding tokens during inference, we randomly replace them with the original learnable queries in the training. For the input of n subjects, the projection processes of different subject images do not affect each other. The resulting n queries will be concatenated and input into the subsequent model as \mathbf{c}_i with $N = n * n_t$ tokens, where n_t is the token quantity per subject.

3.4 Multi-subject Cross-attention

In scenarios involving the generation of multiple subjects, challenges frequently arise that are not exclusive to personalization tasks. These include discordances between subjects and their backgrounds and amongst the subjects themselves. A viable solution to mitigate such conflicts leverages attention masks, contingent upon the availability of layout priors. The incorporation of attention masks within cross-attention mechanisms facilitates the exclusion of padding tokens from the condition, thus minimizing their impact.

To confine the context of each subject to a designated spatial domain, we propose an enhancement to the conventional attention mask, denoted as \mathbf{M} . This adjustment involves the bilateral neglect of tokens within both the query and key matrices, applied specifically for the j th subject as follows:

$$\mathbf{M}_j(x, y) = \begin{cases} 0 & \text{if } [x, y] \in B_j \\ -\infty & \text{if } [x, y] \notin B_j \end{cases} \quad (4)$$

Here, B_j signifies the coordinate set of bounding boxes pertaining to the j th subject. By this means, the conditional image latent $\hat{\mathbf{z}}_{img}$ is derived through:

$$\hat{\mathbf{z}}_{img} = \text{Softmax} \left(\frac{\mathbf{Q}\mathbf{K}_i}{\sqrt{d}} + \mathbf{M} \right) \mathbf{V}_i \quad (5)$$

Herein, \mathbf{M} represents the amalgamation of all subject-specific masks, $\text{Concat}(\mathbf{M}_0, \dots, \mathbf{M}_n)$.

However, an inherent limitation arises when a query patch token is ubiquitously masked across all referenced subjects or remains unmasked (in instances of overlapping bounding boxes), thereby diminishing the intended efficacy of multi-subject cross-attention. To counteract this, we introduce dummy tokens initialized at random preceding the image tokens to symbolize the background. *This strategy is instrumental in ensuring that text conditions predominantly govern areas devoid of any guided layout, thereby considered irrelevant to the referenced images.* Following the acquisition of \mathbf{A} , we apply \mathbf{M}_{bg} to seamlessly mask these tokens within $\hat{\mathbf{z}}_{img}$, as illustrated:

$$\mathbf{z}_{img} = (1 - \mathbf{M}_{bg}) \cdot \hat{\mathbf{z}}_{img} \quad (6)$$

where \mathbf{M}_{bg} is articulated as a binary mask, with elements within the subject bounding boxes designated as zero. **Notably**, certain studies have sought to resolve these conflicts through the application of

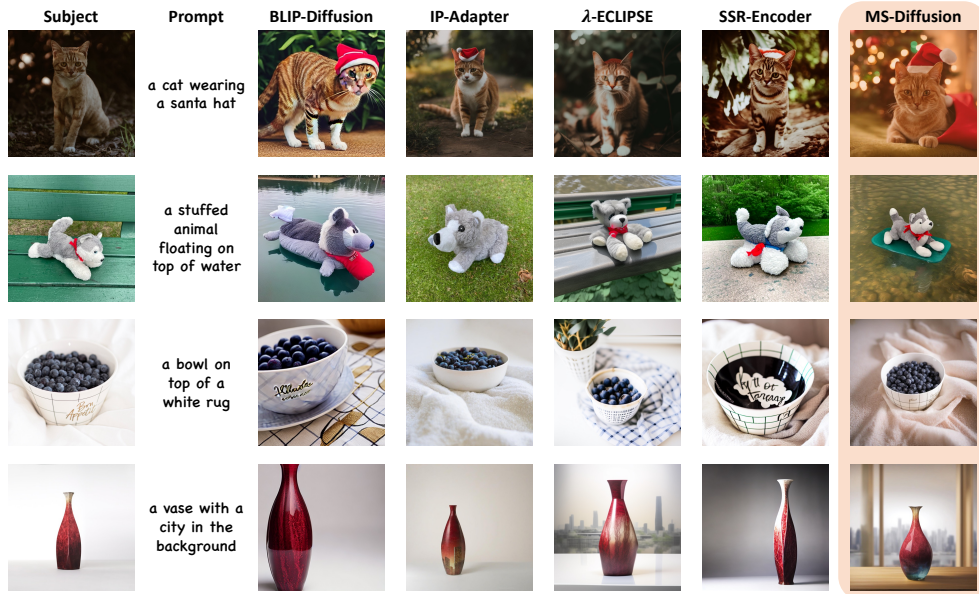


Figure 4: Qualitative results of MS-Diffusion and baselines in single-subject personalization.

Table 2: **Quantitative comparison on MS-Diffusion and baselines.** **Bold** and underline represent the highest and second-highest metrics, respectively. For single-subject, the results for IP-Adapter, Emu2, and Kosmos-G were obtained from [20], while the rest are reported in the corresponding papers. * denotes the model is fine-tuned on DreamBench.

| Method | Single-subject | | | Multi-subject | | | |
|----------------------|----------------|--------------|--------------|---------------|--------------|--------------|--------------|
| | CLIP-I | DINO | CLIP-T | CLIP-I | DINO | M-DINO | CLIP-T |
| Textual Inversion | 0.780 | 0.569 | 0.255 | - | - | - | - |
| DreamBooth | 0.803 | 0.668 | <u>0.305</u> | - | - | - | - |
| BLIP-Diffusion* | 0.805 | 0.670 | 0.302 | - | - | - | - |
| λ -ECLIPSE* | 0.796 | <u>0.682</u> | 0.304 | - | - | - | - |
| MS-Diffusion* | 0.805 | 0.702 | 0.313 | - | - | - | - |
| ELITE | <u>0.771</u> | <u>0.621</u> | <u>0.293</u> | - | - | - | - |
| BLIP-Diffusion | 0.779 | 0.594 | 0.300 | - | - | - | - |
| IP-Adapter | 0.810 | 0.613 | 0.292 | - | - | - | - |
| Emu2 | 0.765 | 0.563 | 0.273 | - | - | - | - |
| Kosmos-G | 0.822 | 0.618 | 0.250 | - | - | - | - |
| λ -ECLIPSE | 0.783 | 0.613 | 0.307 | <u>0.724</u> | 0.419 | 0.094 | <u>0.316</u> |
| SSR-Encoder | <u>0.821</u> | 0.612 | <u>0.308</u> | 0.725 | 0.425 | <u>0.107</u> | 0.303 |
| MS-Diffusion | 0.792 | 0.671 | 0.321 | 0.698 | 0.425 | 0.108 | 0.341 |

objectives on attention maps within the cross-attention mechanism. A series of rigorous experiments have been conducted to substantiate our design, with the details elucidated in Section 4.4.

4 Experiments

4.1 Experiment Setup

Datasets. For training, we utilize an in-house video dataset that contains 3.6M video clips. For evaluation, we measure the single-subject and multi-subject performance on DreamBench [28] and MS-Bench, respectively. DreamBench includes 30 subjects and 25 prompts and we preset all input boxes to [0.25, 0.25, 0.75, 0.75]. To thoroughly assess the performance of multi-subject personalization, we have established a new evaluation standard, MS-Bench, which includes 40

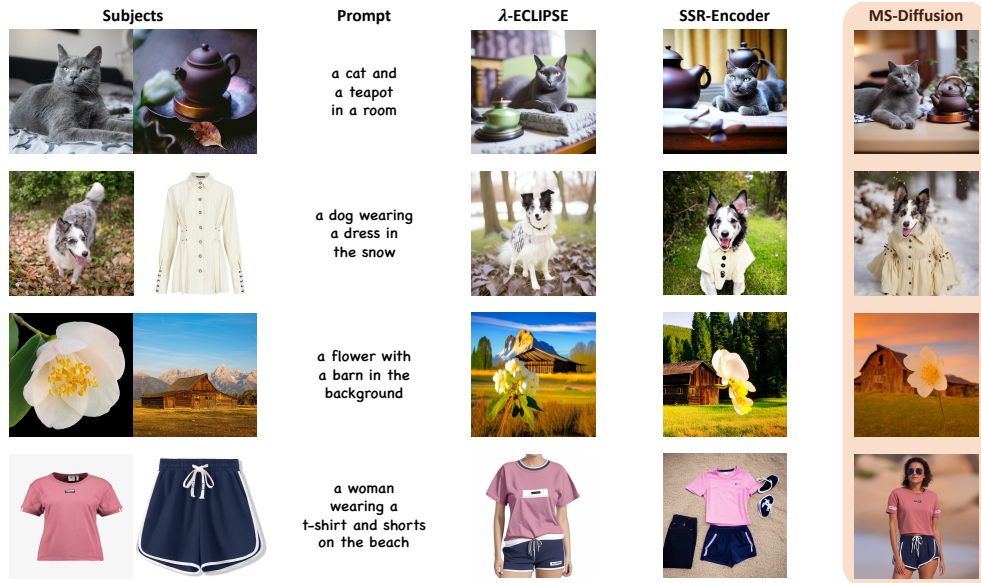


Figure 5: Qualitative results of MS-Diffusion and baselines in multi-subject personalization.

subjects and 1148 combinations, each combination having up to 6 prompts, totaling 4488 distinct test samples. Details of datasets are provided in Section A and Section B.

Evaluation metrics. Following previous works, we measure the performance through image and text fidelity. To assess image fidelity, we employ cosine similarity measures between generated images and subject images within CLIP [25] and DINO [4] spaces, referred to as CLIP-I and DINO, respectively. For text fidelity, we utilize cosine similarity between generated images and text prompts in CLIP space, denoted as CLIP-T. In multi-subject personalization, using the average fidelity to reflect image fidelity is insufficient, as it fails to reveal cases of subject neglect. We further employ the product of multi-subject DINO, denoted as M-DINO, to indicate whether each subject has been recreated in the results.

Baselines. For single-subject personalization, we compare our model with methods mentioned in Table 1. Emu2 [30], Kosmos-G [19], and λ -ECLIPSE [20] are all MLLM-based methods, while λ -ECLIPSE is reported to have better performance. Therefore, we select SSR-Encoder [40] and λ -ECLIPSE [20] as baselines for multi-subject personalization. The implementation details of MS-Diffusion and these methods are contained in Section C.

4.2 Single-subject Comparison

In the single-subject comparison, a detailed examination is carried out utilizing both qualitative and quantitative comparisons to gauge the performance of different methodologies. On the qualitative front, as shown in Figure 4, MS-Diffusion shows an exceptional ability to generate single-subject images with high fidelity and detail retention. In quantitative results provided in Table 2, MS-Diffusion also achieves competitive scores, with obviously the highest DINO and CLIP-T scores at 0.671 and 0.321 respectively on zero-shot scenarios, and leading CLIP-I score of 0.792. For tuning methods, MS-Diffusion outperforms baselines in all metrics. As discussed in [28], DINO more accurately captures the similarity in details between the results and the labels, whereas CLIP-I may exhibit high scores in situations of background overfitting, resulting in a clear advantage for DINO, but a slight disadvantage for CLIP-I of MS-Diffusion.

4.3 Multi-subject Comparison

From a qualitative perspective in Figure 5, MS-Diffusion manages to maintain natural interactions among subjects in generated images while ensuring each subject retains its distinctiveness and

Table 3: **Ablation study of MS-Diffusion.** RS, GRS, MCA, TAL, IAL, and LG represent resampler, grounding resampler, multi-subject cross-attention, text attention loss, image attention loss, and layout guidance, respectively.

| Method | Single-subject | | | Multi-subject | | | |
|---------------------|----------------|--------------|--------------|---------------|--------------|--------------|--------------|
| | CLIP-I | DINO | CLIP-T | CLIP-I | DINO | M-DINO | CLIP-T |
| MS-Diffusion | 0.792 | 0.671 | 0.321 | 0.698 | 0.425 | 0.108 | 0.341 |
| w/o RS | 0.775 | 0.583 | 0.320 | 0.680 | 0.372 | 0.082 | 0.336 |
| w/o GRS | 0.777 | 0.646 | 0.320 | 0.681 | 0.389 | 0.090 | 0.331 |
| w/o MCA | 0.798 | 0.662 | 0.312 | 0.693 | 0.422 | 0.100 | 0.309 |
| w/o LG w/ IAL | 0.761 | 0.577 | 0.284 | 0.675 | 0.377 | 0.080 | 0.305 |
| w/o LG w/ IAL&TAL | 0.809 | 0.660 | 0.293 | 0.687 | 0.413 | 0.093 | 0.316 |

recognizability. Quantitatively, results in Table 2 demonstrate the strength of MS-Diffusion in DINO, M-DINO, and CLIP-T. Unlike in single-subject personalization, there is a larger gap in text fidelity between MS-Diffusion and the baselines in multi-subject personalization, demonstrating that MS-Diffusion not only effectively generates the multiple subjects outlined in the text but also excellently preserves the text control capabilities inherent to SD. Additionally, the image fidelity of MS-Diffusion is comparable, highlighting its superior ability to retain details, particularly significant as low text fidelity is commonly associated with overfitting.

4.4 Ablation Study

Module ablation. We conduct an ablation experiment on the proposed two modules, grounding resampler (GRS) and multi-subject cross-attention (MCA), to validate their effects. For GRS, we replace it with a linear projection layer and a normal resampler [1, 38]. Results in Table 3 indicate that the resampler-like image projector significantly enhances the details, as evidenced by DINO being obviously higher than the linear projector. Moreover, The substantial improvement in multi-object image fidelity by GRS reflects the critical role of the information carried by grounding tokens in multi-object generation. As a key module for resolving conflicts, removing MCA results in a noticeable degradation of text fidelity, especially in multi-subject generation. The combined use of both modules ensures that MS-Diffusion maintains high image and text fidelity simultaneously.

Layout guidance. As mentioned in Section 3.4, we have explored the indispensable role of explicit layout guidance (LG), including grounding tokens and MCA. A straightforward approach to implicitly utilizing layout involves incorporating an attention loss during training. Besides the image attention loss (IAL), we also introduce text attention loss (TAL) to training by setting the original cross-attention layers trainable. The detailed loss definition is provided in Section F. As illustrated in Table 3, an objective to guide the image cross-attention helps the personalization hardly at all. TAL has somewhat resolved the conflict issues, but its performance is inferior to MS-Diffusion while introducing additional training parameters. We consider the inclusion of LG necessary and rational, not merely for the performance enhancements it offers, but also because it effectively resolves the various multi-object generation issues highlighted in Figure 2.

5 Conclusion

This study makes a significant contribution to the field of P-T2I diffusion models with the development of MS-Diffusion. This zero-shot framework excels at capturing intricate subject details and smoothly blending multiple subjects into a single coherent image. Equipped with the innovative Grounding Resampler and Multi-subject Cross-attention mechanisms, our model effectively overcomes common multi-subject personalization issues, such as subject neglect and conflict. Extensive ablation studies underscore MS-Diffusion’s enhanced performance in image synthesis fidelity compared to existing models. It stands as a groundbreaking approach for P-T2I applications that are free from the need for fine-tuning and require layout guidance.

References

- [1] Jean-Baptiste Alayrac, Jeff Donahue, Pauline Luc, Antoine Miech, Iain Barr, Yana Hasson, Karel Lenc, Arthur Mensch, Katherine Millican, Malcolm Reynolds, Roman Ring, Eliza Rutherford, Serkan Cabi, Tengda Han, Zhitao Gong, Sina Samangooei, Marianne Monteiro, Jacob L. Menick, Sebastian Borgeaud, Andy Brock, Aida Nematzadeh, Sahand Sharifzadeh, Mikolaj Binkowski, Ricardo Barreira, Oriol Vinyals, Andrew Zisserman, and Karén Simonyan. Flamingo: a visual language model for few-shot learning. In *NeurIPS*, 2022.
- [2] Fan Bao, Shen Nie, Kaiwen Xue, Yue Cao, Chongxuan Li, Hang Su, and Jun Zhu. All are worth words: A vit backbone for diffusion models. In *CVPR*, pages 22669–22679. IEEE, 2023.
- [3] James Betker, Gabriel Goh, Li Jing, Tim Brooks, Jianfeng Wang, Linjie Li, Long Ouyang, Juntang Zhuang, Joyce Lee, Yufei Guo, et al. Improving image generation with better captions. *Computer Science*. <https://cdn.openai.com/papers/dall-e-3.pdf>, 2:3, 2023.
- [4] Mathilde Caron, Hugo Touvron, Ishan Misra, Hervé Jégou, Julien Mairal, Piotr Bojanowski, and Armand Joulin. Emerging properties in self-supervised vision transformers. In *ICCV*, 2021.
- [5] Junsong Chen, Jincheng Yu, Chongjian Ge, Lewei Yao, Enze Xie, Yue Wu, Zhongdao Wang, James T. Kwok, Ping Luo, Huchuan Lu, and Zhenguo Li. Pixart- α : Fast training of diffusion transformer for photorealistic text-to-image synthesis. *CoRR*, abs/2310.00426, 2023.
- [6] Xi Chen, Lianghua Huang, Yu Liu, Yujun Shen, Deli Zhao, and Hengshuang Zhao. Anydoor: Zero-shot object-level image customization. *CoRR*, abs/2307.09481, 2023.
- [7] Hyung Won Chung, Le Hou, Shayne Longpre, Barret Zoph, Yi Tay, William Fedus, Yunxuan Li, Xuezhi Wang, Mostafa Dehghani, Siddhartha Brahma, et al. Scaling instruction-finetuned language models. *arXiv preprint arXiv:2210.11416*, 2022.
- [8] Alexey Dosovitskiy, Lucas Beyer, Alexander Kolesnikov, Dirk Weissenborn, Xiaohua Zhai, Thomas Unterthiner, Mostafa Dehghani, Matthias Minderer, Georg Heigold, Sylvain Gelly, Jakob Uszkoreit, and Neil Houlsby. An image is worth 16x16 words: Transformers for image recognition at scale. In *ICLR*. OpenReview.net, 2021.
- [9] Rinon Gal, Yuval Alaluf, Yuval Atzmon, Or Patashnik, Amit Haim Bermano, Gal Chechik, and Daniel Cohen-Or. An image is worth one word: Personalizing text-to-image generation using textual inversion. In *ICLR*. OpenReview.net, 2023.
- [10] Ligong Han, Yinxiao Li, Han Zhang, Peyman Milanfar, Dimitris N. Metaxas, and Feng Yang. Svdiff: Compact parameter space for diffusion fine-tuning. In *ICCV*, pages 7289–7300. IEEE, 2023.
- [11] Amir Hertz, Ron Mokady, Jay Tenenbaum, Kfir Aberman, Yael Pritch, and Daniel Cohen-Or. Prompt-to-prompt image editing with cross-attention control. In *ICLR*. OpenReview.net, 2023.
- [12] Yunji Kim, Jiyoung Lee, Jin-Hwa Kim, Jung-Woo Ha, and Jun-Yan Zhu. Dense text-to-image generation with attention modulation. In *ICCV*, 2023.
- [13] Alexander Kirillov, Eric Mintun, Nikhila Ravi, Hanzi Mao, Chloé Rolland, Laura Gustafson, Tete Xiao, Spencer Whitehead, Alexander C. Berg, Wan-Yen Lo, Piotr Dollár, and Ross B. Girshick. Segment anything. In *ICCV*, pages 3992–4003. IEEE, 2023.
- [14] Nupur Kumari, Bingliang Zhang, Richard Zhang, Eli Shechtman, and Jun-Yan Zhu. Multi-concept customization of text-to-image diffusion. In *CVPR*, pages 1931–1941. IEEE, 2023.
- [15] Dongxu Li, Junnan Li, and Steven C. H. Hoi. Blip-diffusion: Pre-trained subject representation for controllable text-to-image generation and editing. In *NeurIPS*, 2023.
- [16] Junnan Li, Dongxu Li, Silvio Savarese, and Steven C. H. Hoi. BLIP-2: bootstrapping language-image pre-training with frozen image encoders and large language models. In *ICML*, volume 202 of *Proceedings of Machine Learning Research*, pages 19730–19742. PMLR, 2023.
- [17] Yuheng Li, Haotian Liu, Qingyang Wu, Fangzhou Mu, Jianwei Yang, Jianfeng Gao, Chunyuan Li, and Yong Jae Lee. Gligen: Open-set grounded text-to-image generation. *CVPR*, 2023.
- [18] Shilong Liu, Zhaoyang Zeng, Tianhe Ren, Feng Li, Hao Zhang, Jie Yang, Chunyuan Li, Jianwei Yang, Hang Su, Jun Zhu, et al. Grounding dino: Marrying dino with grounded pre-training for open-set object detection. *arXiv preprint arXiv:2303.05499*, 2023.

- [19] Xichen Pan, Li Dong, Shaohan Huang, Zhiliang Peng, Wenhui Chen, and Furu Wei. Kosmos-g: Generating images in context with multimodal large language models. *CoRR*, abs/2310.02992, 2023.
- [20] Maitreya Patel, Sangmin Jung, Chitta Baral, and Yezhou Yang. λ -eclipse: Multi-concept personalized text-to-image diffusion models by leveraging CLIP latent space. *CoRR*, abs/2402.05195, 2024.
- [21] William Peebles and Saining Xie. Scalable diffusion models with transformers. In *ICCV*, pages 4172–4182. IEEE, 2023.
- [22] Pablo Pernias, Dominic Rampas, Mats Leon Richter, Christopher Pal, and Marc Aubreville. Würstchen: An efficient architecture for large-scale text-to-image diffusion models. In *The Twelfth International Conference on Learning Representations*, 2023.
- [23] Dustin Podell, Zion English, Kyle Lacey, Andreas Blattmann, Tim Dockhorn, Jonas Müller, Joe Penna, and Robin Rombach. SDXL: improving latent diffusion models for high-resolution image synthesis. *CoRR*, abs/2307.01952, 2023.
- [24] Zeju Qiu, Weiyang Liu, Haiwen Feng, Yuxuan Xue, Yao Feng, Zhen Liu, Dan Zhang, Adrian Weller, and Bernhard Schölkopf. Controlling text-to-image diffusion by orthogonal finetuning. In *NeurIPS*, 2023.
- [25] Alec Radford, Jong Wook Kim, Chris Hallacy, Aditya Ramesh, Gabriel Goh, Sandhini Agarwal, Girish Sastry, Amanda Askell, Pamela Mishkin, Jack Clark, Gretchen Krueger, and Ilya Sutskever. Learning transferable visual models from natural language supervision. In *ICML*, volume 139 of *Proceedings of Machine Learning Research*, pages 8748–8763. PMLR, 2021.
- [26] Anton Razhigaev, Arseniy Shakhmatov, Anastasia Maltseva, Vladimir Arkhipkin, Igor Pavlov, Ilya Ryabov, Angelina Kuts, Alexander Panchenko, Andrey Kuznetsov, and Denis Dimitrov. Kandinsky: An improved text-to-image synthesis with image prior and latent diffusion. In *EMNLP*, pages 286–295. Association for Computational Linguistics, 2023.
- [27] Robin Rombach, Andreas Blattmann, Dominik Lorenz, Patrick Esser, and Björn Ommer. High-resolution image synthesis with latent diffusion models. In *CVPR*, pages 10674–10685. IEEE, 2022.
- [28] Nataniel Ruiz, Yuanzhen Li, Varun Jampani, Yael Pritch, Michael Rubinstein, and Kfir Aberman. Dream-booth: Fine tuning text-to-image diffusion models for subject-driven generation. In *CVPR*, pages 22500–22510. IEEE, 2023.
- [29] Chitwan Saharia, William Chan, Saurabh Saxena, Lala Li, Jay Whang, Emily L. Denton, Seyed Kamyar Seyed Ghasemipour, Raphael Gontijo Lopes, Burcu Karagol Ayan, Tim Salimans, Jonathan Ho, David J. Fleet, and Mohammad Norouzi. Photorealistic text-to-image diffusion models with deep language understanding. In *NeurIPS*, 2022.
- [30] Quan Sun, Yufeng Cui, Xiaosong Zhang, Fan Zhang, Qiying Yu, Zhengxiong Luo, Yueze Wang, Yongming Rao, Jingjing Liu, Tiejun Huang, and Xinlong Wang. Generative multimodal models are in-context learners. *CoRR*, abs/2312.13286, 2023.
- [31] Raphael Tang, Linqing Liu, Akshat Pandey, Zhiying Jiang, Gefei Yang, Karun Kumar, Pontus Stenetorp, Jimmy Lin, and Ferhan Ture. What the DAAM: interpreting stable diffusion using cross attention. In *ACL*, pages 5644–5659. Association for Computational Linguistics, 2023.
- [32] Aäron van den Oord, Oriol Vinyals, and Koray Kavukcuoglu. Neural discrete representation learning. In *NeurIPS*, pages 6306–6315, 2017.
- [33] Qixun Wang, Xu Bai, Haofan Wang, Zekui Qin, and Anthony Chen. Instantid: Zero-shot identity-preserving generation in seconds. *arXiv preprint arXiv:2401.07519*, 2024.
- [34] Xudong Wang, Trevor Darrell, Sai Saketh Rambhatla, Rohit Girdhar, and Ishan Misra. Instancediffusion: Instance-level control for image generation. *CoRR*, abs/2402.03290, 2024.
- [35] Zirui Wang, Zhizhou Sha, Zheng Ding, Yilin Wang, and Zhuowen Tu. Tokencompose: Grounding diffusion with token-level supervision. *CoRR*, abs/2312.03626, 2023.
- [36] Yuxiang Wei, Yabo Zhang, Zhilong Ji, Jinfeng Bai, Lei Zhang, and Wangmeng Zuo. ELITE: encoding visual concepts into textual embeddings for customized text-to-image generation. In *ICCV*, pages 15897–15907. IEEE, 2023.
- [37] Zhichao Wei, Qingkun Su, Long Qin, and Weizhi Wang. Mm-diff: High-fidelity image personalization via multi-modal condition integration. *CoRR*, abs/2403.15059, 2024.

- [38] Hu Ye, Jun Zhang, Sibao Liu, Xiao Han, and Wei Yang. Ip-adapter: Text compatible image prompt adapter for text-to-image diffusion models. *CoRR*, abs/2308.06721, 2023.
- [39] Lvmin Zhang, Anyi Rao, and Maneesh Agrawala. Adding conditional control to text-to-image diffusion models. In *IEEE/CVF International Conference on Computer Vision, ICCV 2023, Paris, France, October 1-6, 2023*, pages 3813–3824. IEEE, 2023.
- [40] Yuxuan Zhang, Jiaming Liu, Yiren Song, Rui Wang, Hao Tang, Jinpeng Yu, Huaxia Li, Xu Tang, Yao Hu, Han Pan, and Zhongliang Jing. Ssr-encoder: Encoding selective subject representation for subject-driven generation. *CoRR*, abs/2312.16272, 2023.
- [41] Guangcong Zheng, Xianpan Zhou, Xuewei Li, Zhongang Qi, Ying Shan, and Xi Li. Layoutdiffusion: Controllable diffusion model for layout-to-image generation. In *CVPR*, pages 22490–22499. IEEE, 2023.
- [42] Dewei Zhou, You Li, Fan Ma, Zongting Zhang, and Yi Yang. MIGC: multi-instance generation controller for text-to-image synthesis. *CoRR*, abs/2402.05408, 2024.

A Training Dataset Construction Pipeline

Figure 6 illustrates the construction pipeline of the training dataset. Firstly, we randomly select two frames from a video clip, one as the reference and the other as the ground truth. Both frames are captioned by BLIP-2 [16]. Secondly, we utilize a NER model² to extract entities from the caption. Entities and images are then input into Grounding DINO [18] to obtain the boxes, which are parts of the final input of the model. Taking the boxes as prompts of SAM [13], we can further obtain segmentation masks to extract subjects from the reference image. Since the entities in different frames can be different, we design a subject matcher, which finds the correspondence between the frames by conducting Hungarian Algorithm on the entity image embeddings. Frames in a video typically contain the same entities but exhibit clear differences in details such as angles and poses. This makes them highly suitable as training data for personalized image generation models, which can help mitigate the model’s tendency to copy-and-paste.

Our dataset comprises 2.8M general scenario videos and 0.8M product demonstration videos, where the former covers more scenarios and the latter has more clear subjects. 2-5 frames for each are adopted in the training. In practice, there may only be 1-2 subjects successfully matched. To ensure that the training data contains a sufficient number of reference subjects, for the targets where matching fails, we directly use the corresponding parts of the ground truth as references. Subjects that are too small, too large, or have imbalanced proportions are filtered out. Each training sample can have up to 4 subjects, and we pad in the ones with fewer than 4.

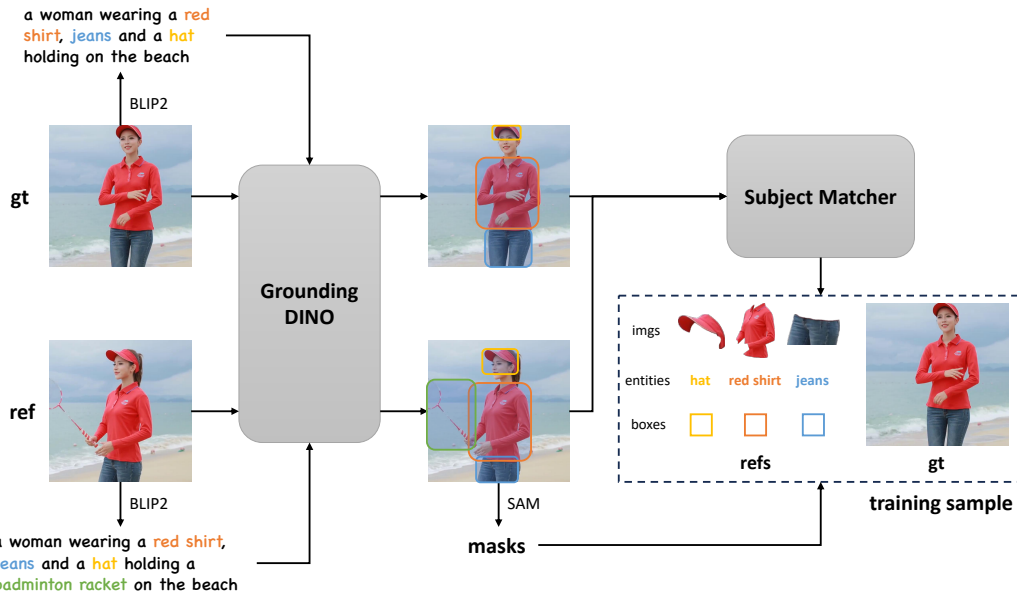


Figure 6: **Data construction pipeline of our work.** For the input of two frames, we can get subject images, entities, and boxes. Note that the entities and boxes are from the ground truth frame since they indicate the information in the generated result.

B Details of MS-Bench

To construct MS-Bench, we collect subjects from [9, 14, 28], the Internet³, and an internal dataset that does not overlap with the training set. MS-Bench contains four data types and 13 combination types with two or three subjects. We provide the details in Table 4. Each combination type other than those related to the scene has 6 prompt variations. There are 1148 combinations and 4488 evaluation samples, where entities and boxes are subject categories and preset layouts. Compared to

²<https://spacy.io/>

³<https://unsplash.com/>

Table 4: **Explanation of MS-Bench.** Each combination type has preset prompts and boxes. [S] represents prompt variations about the scene, including "in a room", "in the jungle", "in the snow", "on the beach", "on the grass", and "on a cobblestone street".

| Type | Prompt | Boxes |
|---|---|--|
| living+living living+object object+object | a {0} and a {1} [S] | [0.00, 0.25, 0.50, 0.75] [0.50, 0.25, 1.00, 0.75] |
| living+upwearing | a {0} wearing a {1} [S] | [0.25, 0.25, 0.75, 0.75] [0.25, 0.00, 0.75, 0.25] |
| living+midwearing living+wholewearing | a {0} wearing a {1} [S] | [0.25, 0.25, 0.75, 0.75] [0.25, 0.25, 0.75, 0.75] |
| midwearing+downwearing | a woman wearing a {0} and a {1} [S] | [0.25, 0.25, 0.75, 0.60] [0.25, 0.60, 0.75, 1.00] |
| living+scene object+scene | a {0} with a {1} in the background | [0.25, 0.25, 0.75, 0.75] [0.00, 0.00, 1.00, 1.00] |
| living+living+living object+object+object | a {0}, a {1}, and a {2} [S] | [0.00, 0.25, 0.35, 0.75] [0.35, 0.25, 0.65, 0.75] [0.65, 0.25, 1.00, 0.75] |
| living+object+scene | a {0} and a {1} with a {2} in the background | [0.00, 0.25, 0.50, 0.75] [0.50, 0.25, 1.00, 0.75] [0.00, 0.00, 1.00, 1.00] |
| upwearing+midwearing+ downwearing | a woman wearing a {0}, a {1}, and a {2} [S] | [0.25, 0.00, 0.75, 0.25] [0.25, 0.25, 0.75, 0.60] [0.25, 0.60, 0.75, 1.00] |

other multi-subject benchmarks, our MS-Bench ensures that the model performance can be reflected comprehensively in abundant cases.

C Experiment Settings

Training and Inference. The pre-trained model employed in MS-Diffusion is Stable Diffusion XL (SDXL) [23]. Implemented by Pytorch 2.0.1 and Diffusers 0.23.1, our model is trained on 16 A100 GPUs for 120k steps with a batch size of 8 and a learning rate of $1e-4$. Following the training of [38], we set $\gamma = 1.0$ in cross-attention layers and dropped the text and image condition using the same probability. To ensure the model is not dependent on the grounding tokens (Section 3.3), we also randomly drop them with a probability of 0.1. We generate five images for each sample during the inference, with unconditional guidance scale and γ set to 7.5 and 0.6, respectively, to get better results.

Comparative methods. Here we provide the details of the baselines compared in qualitative and quantitative experiments:

- **BLIP-Diffusion** [15] utilizes BLIP-2 [16] to unite the text and image embeddings. We implement it in the qualitative comparison using Diffusers.
- **IP-Adapter** [38] also uses image prompt as the condition. We run qualitative samples on their official code with the scale set to 0.5 recommended by the paper. Considering fairness, we use the result of SDXL in Table 2.
- **SSR-Encoder** [40] design a query network to extract the specified subject of a single image, which enables it to finish multi-subject generation. We leverage it as one of the baselines in multi-subject personalization. For performance comparison, we employed the official code provided, alongside the default hyperparameters specified in the code repository.

- λ -ECLIPSE [20] trains an independent multi-modal encoder and employs Kandinsky as the generative backbone. Since it outperforms other MLLM-based approaches, we choose it to be the representative. To facilitate a comparative analysis of performance, the study utilized the officially provided code, in conjunction with the default hyperparameters delineated within the corresponding code repository.

D More Results of Single-subject Personalization

Additional qualitative results on DreamBench are provided in Figure 8. MS-Diffusion shows excellent text fidelity in all subjects while keeping subject details, especially the living ones (dogs). It can be noticed that some elements in the background (the third line and the fourth line) also occur in the results (the grass and the teapot holder) since the entire images are referenced during the generation. Their scope of action depends on the input bounding box. In practical applications, using masked images as a condition is recommended.

E More Results of Multi-subject Personalization

We provide additional multi-subject personalized images based on MS-Bench in Figure 9. The results encompass various combination types, fully demonstrating the generalizability and robustness of MS-Diffusion. When the scene changes freely according to the text, the details of the subject are preserved without being affected. In addition to common parallel combinations, MS-Diffusion also performs well in personalized generation for combinations with certain overlapping areas, such as "living+midwearing" and "object+scene".

F Layout Guidance

Cross-attention maps can intuitively reflect the condition-image attribution relation [11, 31]. Recent works [35, 37] have studied utilizing an objective on the cross-attention maps in multi-subject generation. The objective exists only in training, considered implicit and insufficient to handle multi-subject conflicts. We have provided the performance comparison between our explicit layout guidance and attention loss in Section 4.4. For a single cross-attention layer, the attention loss of the j th subject is calculated by:

$$\mathcal{L}_{am}^j = \left(1 - \frac{\sum_{[x,y] \in B_j} \mathbf{A}_{[x,y],j}}{\sum_{[x,y]} \mathbf{A}_{[x,y],j}} \right)^2 \quad (7)$$

where $[x, y]$ corresponds to a latent token in \mathbf{Q} and B_j is the bounding box of the j th subject. This objective aims to promote the activation of attention maps within specific boxes. We average \mathcal{L}_{am}^j across layers and subjects and set its weight to 0.01 in the final loss. To validate the text attention loss, we also optimize the text cross-attention layers in training, increasing approximately 70% in learnable parameters.

Although our model provides explicit layout guidance, it still significantly differs from layout-based diffusion. Firstly, the information of boxes in the grounding resampler is prior, and its conditional effect is relatively weak. We have also reduced the model’s reliance on this input by randomly dropping grounding tokens. Secondly, the multi-subject cross-attention only exists in image cross-attention, inherently controlling the action of image conditions in specified areas, but cannot determine the whole generation of the diffusion model. Our goal is not to develop a method that fully supports layout control but to utilize layout information to guide the model in resolving conflicts in multi-subject generation.

To further explore the layout control capability of MS-Diffusion, we provide qualitative results in Figure 10. It can be demonstrated that MS-Diffusion can generate images that adhere to layout conditions, even in the case of two instances of the same category. However, the generated positions are not entirely accurate, especially in "a cat and a cat on the grass", illustrating that the layout condition is relatively weak compared to text and image prompts in the personalization task.

G Integration with ControlNet

In the realm of text-to-image diffusion models, a notable application is the enhancement of structural control within image generation. Our MS-Diffusion maintains the original network architecture unchanged, thus ensuring full compatibility with existing controllable tools. Consequently, this allows for the generation of images that are not only prompted by images but also governed by additional conditions. By integrating our MS-Diffusion with established controllable mechanisms such as ControlNet, we demonstrate the capacity to produce images under varied structural directives. Figure 11 displays an array of images synthesized with image prompts coupled with distinct structural controls (depth, canny edge, openpose). This seamless cooperation between our method and these tools facilitates the creation of highly controllable images without necessitating fine-tuning.

H Text-Image Attribution Analysis

In MS-Diffusion, our focus is primarily on resolving conflicts between subjects without altering the control mechanism of the text. While some approaches [12, 34, 35, 42] in non-personalized text-to-image tasks address multi-object generation conflicts through text cross-attention, this inevitably requires tuning the diffusion model’s parameters, thereby affecting the plug-and-play nature, which is not preferred by us. As demonstrated in the text-image attribution analysis presented in Figure 7, the control of multiple objects by text in our model is also quite evident. This may be related to the explicit layout guidance for subjects, since the images and text condition jointly in the generation process. We also attempted to control text cross-attention using the same mechanism as in Section 3.4, but no differences were observed in the results.



Figure 7: Text-image attribution analysis of MS-Diffusion. We average the attention maps corresponding to the subjects and translate them to normalized heat maps.

I Subject Interpolation

The blending of two distinct subject representations to yield composite subjects with hybrid characteristics is feasible through the navigation of the embedding space linking the subjects. As depicted in Figure 12, linear interpolations are conducted among dog and hat representations, subsequently rendering the interpolated subject in an unaccustomed context. The visualization reveals a natural gradation of subject appearance along the interpolated trajectory that harmonizes with the surrounding environment. This technique proves beneficial when applied in subject fusion and style transfer.

J Limitations

There are certain limitations in MS-Diffusion. The box-based indication of positions lacks precision, making it challenging to work effectively when the interaction between subjects is stronger. Moreover, the model requires explicit layout input during inference, and generating complex scenes becomes difficult. Though MS-Diffusion beats SOTA personalized diffusion methods in both single-subject and multi-subject generation, it still suffers from the influence of background in subject images. In the future, we will tackle the above limitations and extend the model to more applications.

K Societal Impact

As an image personalization method, MS-Diffusion aims to customize images based on user-provided subjects without fine-tuning. Additionally, the multi-subject reference capability of MS-Diffusion allows users to freely combine and re-create different concepts. However, MS-Diffusion can also be used to generate deceptive images, especially those involving subject combinations that would not exist in reality, an issue that remains to be addressed in the future.

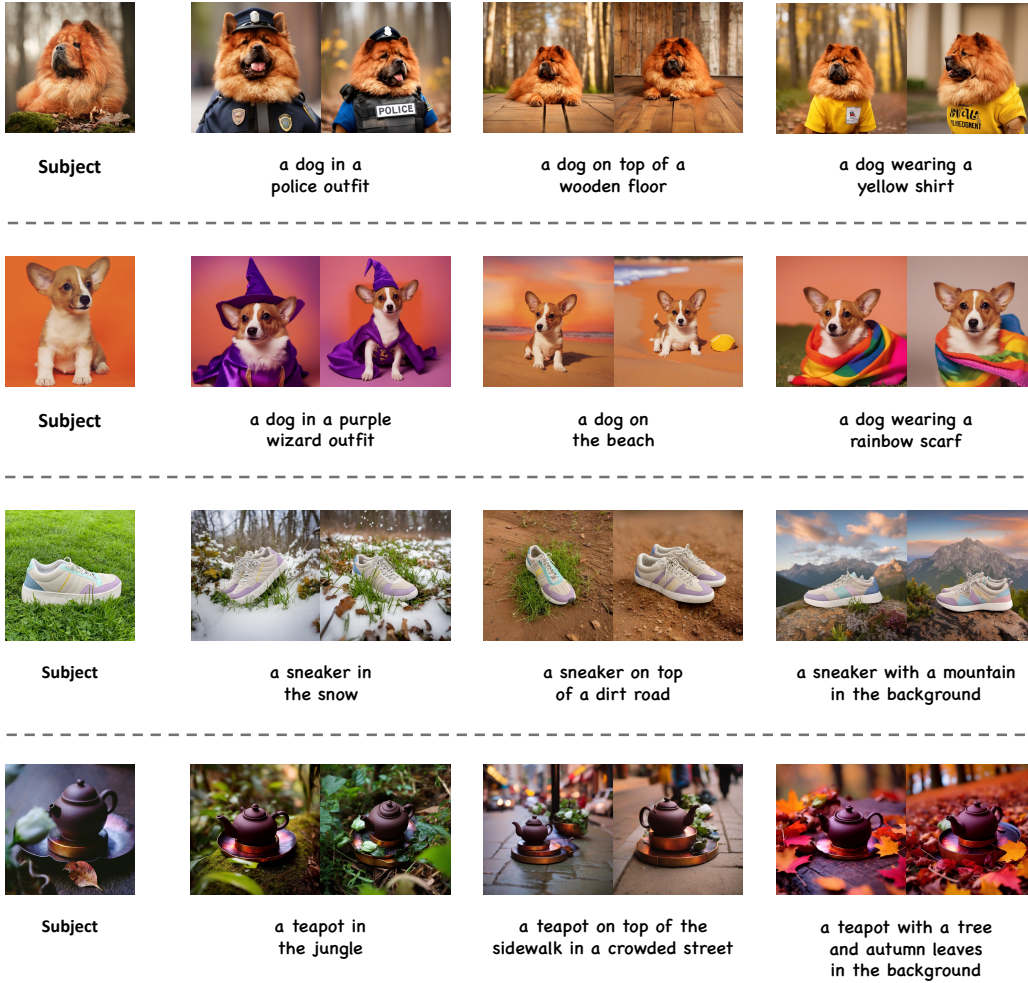


Figure 8: Additional qualitative results of MS-Diffusion in single-subject personalization.



Figure 9: Additional qualitative results of MS-Diffusion in multi-subject personalization.

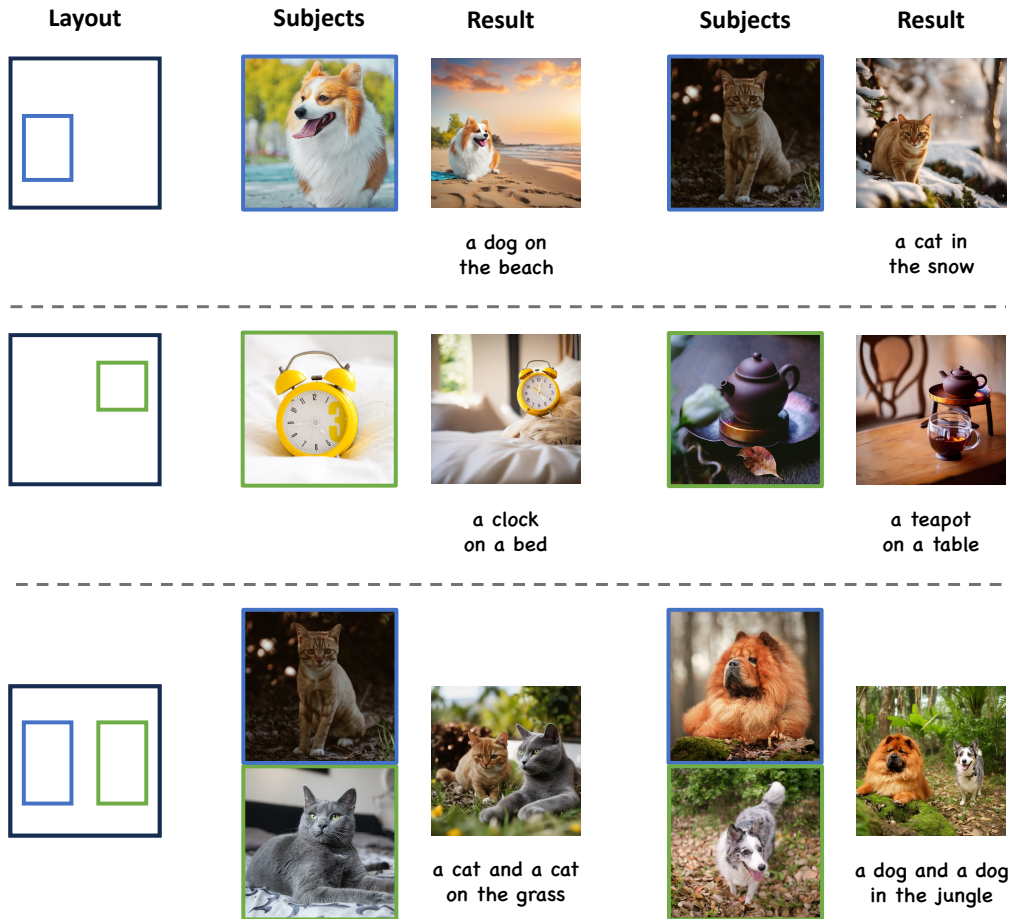


Figure 10: Qualitative examples of MS-Diffusion about the layout control ability. Bounding boxes of different colors correspond to subjects with different color borders.

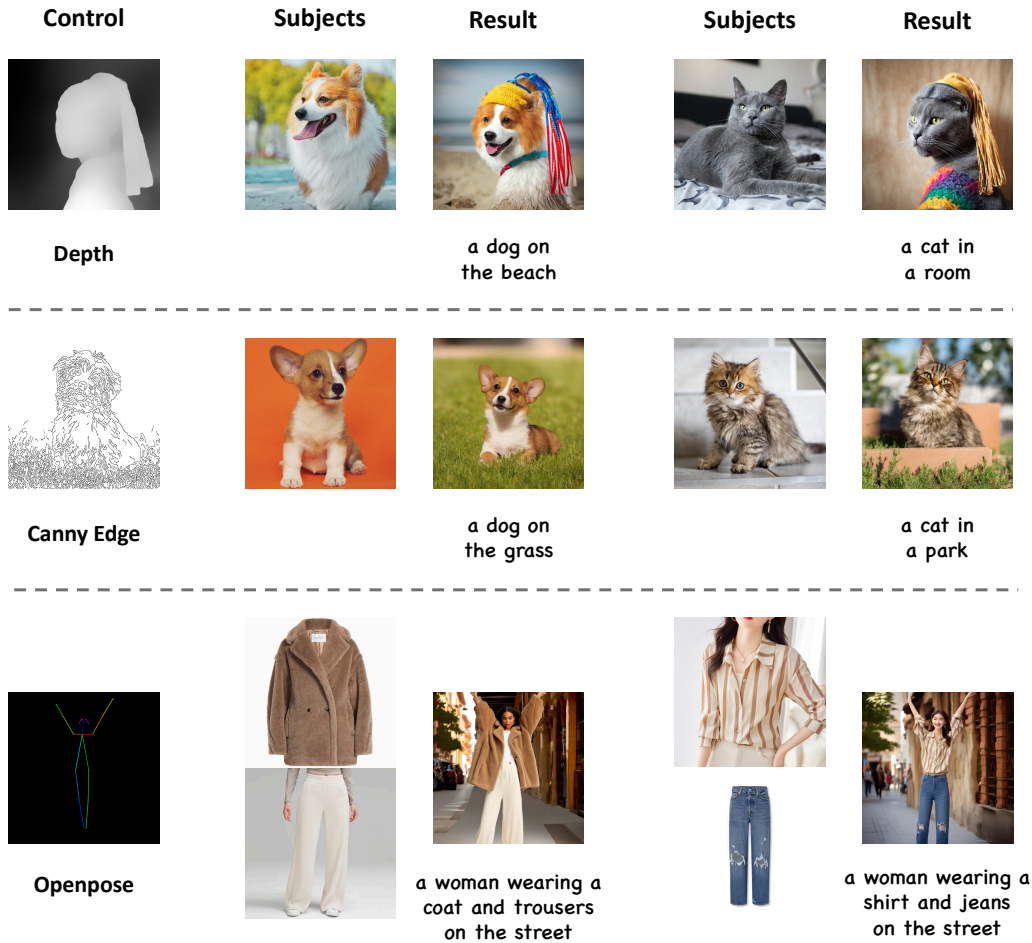


Figure 11: Generative results when integrating different control conditions. The integrated Control-Nets are composed of depth, canny edge, and openpose.

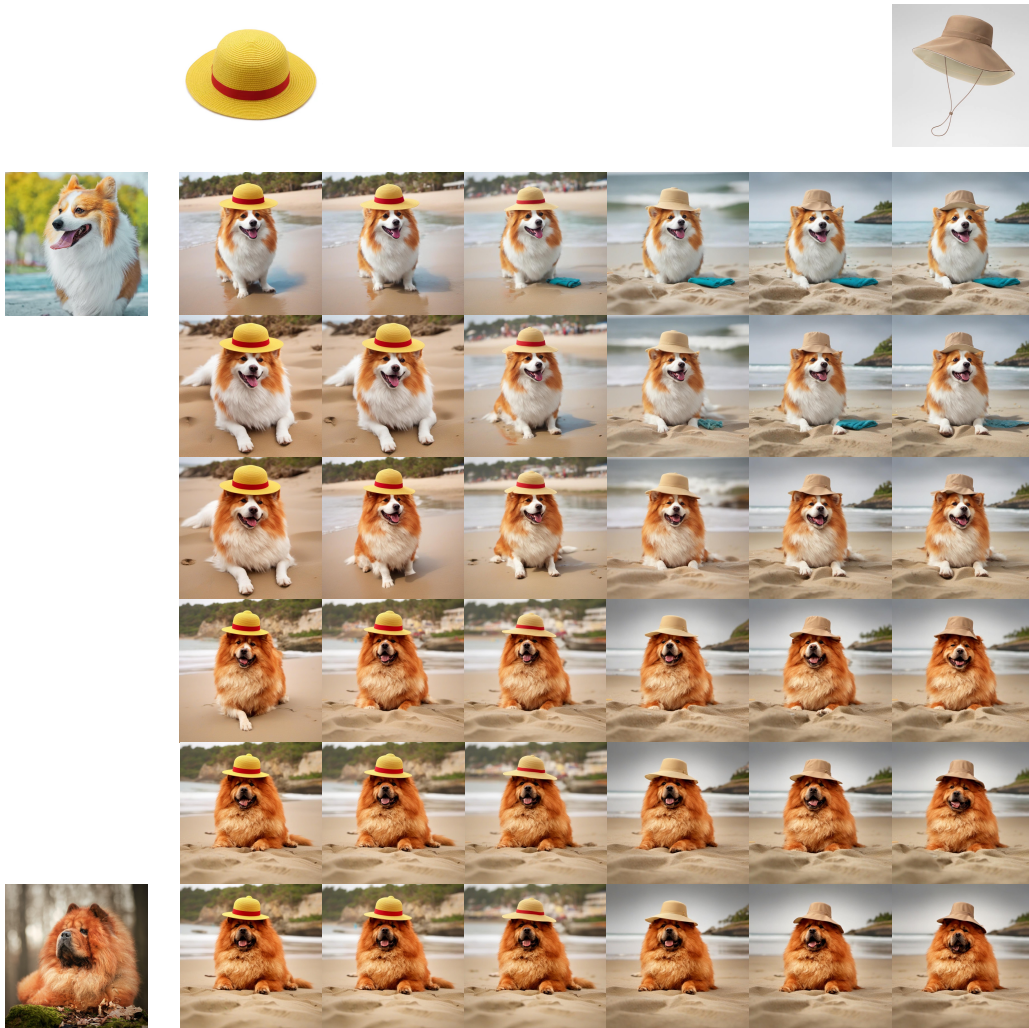


Figure 12: Subjects interpolation in multi-subject generation. We select two dogs and two hats to conduct linear interpolation with the text set to "a dog wearing a hat on the beach".